Supporting information for: First-principles parameterization of polarizable coarse-grained force fields for ionic liquids

Frank Uhlig,* Johannes Zeman, Jens Smiatek, and Christian Holm

Institute for Computational Physics, University of Stuttgart, D-70569 Stuttgart, Germany

E-mail: fuhlig@icp.uni-stuttgart.de

Phone: +49(0)711/685-63607. Fax: +49(0)711/685-63658

1 Input structures and nomenclature

The atomistic input structures for our force field parametrization were taken from the CL&P force field.[S1,S2] Figure S1 depicts the structure and corresponding atom types of the CL&P force field used for the bonded interactions.

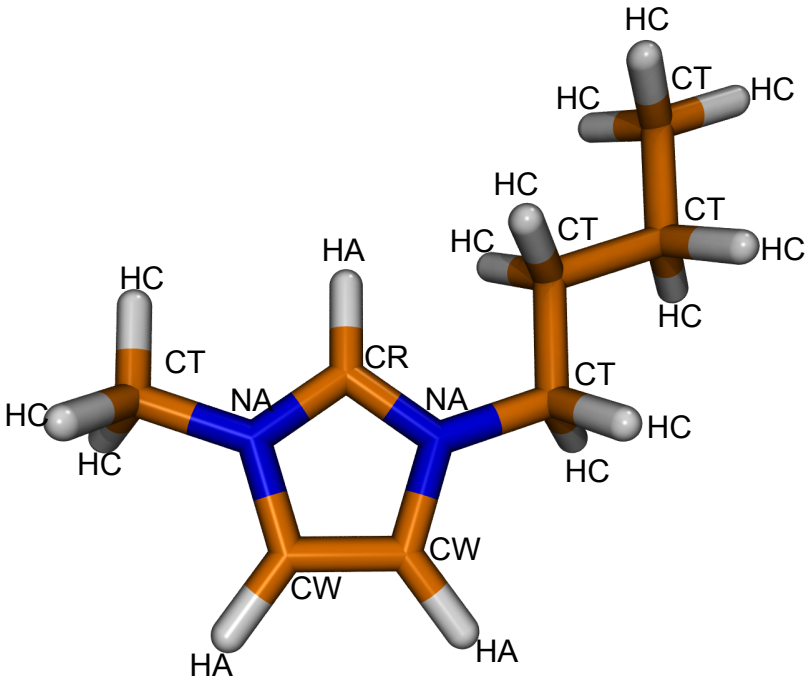

Figure S1: Structure of $C_4C_1Im^+$ cation and corresponding atom types as defined in the CL&P force field.[S1,S2]

We performed ab initio molecular dynamics simulations as described in the main article. From these simulations we extracted average values of bonds and angles and compare them to the equilibrium values from the CL&P force field. All values are listed in Tab. S1.

Table S1: Comparison between parameters for bonds and bond angles in current work and CLaP force field.[S1,S2] Types are denoted in the model in Fig. S1.

bond/angle	current work	CLaP
BONDS		
HC CT	1.0986	1.090
CT CT	1.5404	1.529
CR HA	1.0829	1.080
CW HA	1.0827	1.080
CR NA	1.3485	1.315
CW NA	1.3914	1.378
CW CW	1.3707	1.341
NA CT	1.4781	1.466
P F	1.656	1.606
ANGLES		
CT CT CT	113.063	112.7
CT CT HC	109.797	110.7
CW NA CR	108.838	108.0
CW NA CT	125.436	125.6
CR NA CT	124.981	126.4
NA CR HA	125.316	125.1
NA CR NA	108.054	109.8
NA CW CW	106.921	107.1
NA CW HA	121.572	122.0
CW CW HA	130.815	130.9
NA CT HC	107.968	110.7
NA CT CT	112.394	112.7

Bond lengths and angles agree well between CL&P force field and ab initio simulations. This indicates that the structures of the CL&P force field are representative of the bulk liquid structure. Hence, we use the structures from this force field throughout our parametrization. In the following, (x, y, z)-coordinates of ions used in parametrization of polarizable force fields are given. All values are in Å.

$C_2C_1Im^+$ cation:

```
N 0.000000 0.000000 0.000000
C 1.315000 0.000000 0.000000
N 1.760440 1.237258 0.000000
```

C 0.671607 2.081844 0.000000

C -0.425532 1.310762 0.000000

C -0.870246 -1.179758 0.000000

H 1.936006 -0.883602 0.000000

C 3.166070 1.653625 0.000000

H 0.697051 3.161544 0.000000

H -1.450020 1.652557 0.000000

H -1.499664 -1.167599 -0.889823

H -0.259374 -2.082496 -0.000000

H -1.499664 -1.167599 0.889823

C 4.059504 0.423919 0.000000

H 3.369026 2.249547 -0.889823

H 3.369026 2.249547 0.889823

H 5.104617 0.733496 0.000000

H 3.857745 -0.172410 0.889823

H 3.857745 -0.172410 -0.889823

$C_4C_1Im^+$ cation:

N 0.000000 0.000000 0.000000

C 1.315000 0.000000 0.000000

N 1.760440 1.237258 0.000000

C 0.671607 2.081844 0.000000

C -0.425532 1.310762 0.000000

C -0.870246 -1.179758 0.000000

H 1.936006 -0.883602 0.000000

C 3.166070 1.653625 0.000000

H 0.697051 3.161544 0.000000

H -1.450020 1.652557 0.000000

H -1.499664 -1.167599 -0.889823

H -0.259374 -2.082496 -0.000000

H -1.499664 -1.167599 0.889823

C 4.064794 0.416638 0.000000

H 3.369026 2.249547 -0.889823

H 3.369026 2.249547 0.889823

C 5.530829 0.850897 0.000000

H 3.863035 -0.179691 0.889823

H 3.863035 -0.179691 -0.889823

C 6.429553 -0.386090 0.000000

H 5.733785 1.446820 0.889823

H 5.733785 1.446820 -0.889823

H 7.474666 -0.076513 0.000000

H 6.227794 -0.982419 -0.889823

H 6.227794 -0.982419 0.889823

$C_6C_1Im^+$ cation:

N 0.000000 0.000000 0.000000

C 1.315000 0.000000 0.000000

N 1.760440 1.237258 0.000000

C 0.671607 2.081844 0.000000

C -0.425532 1.310762 0.000000

C -0.870246 -1.179758 0.000000

H 1.936006 -0.883602 0.000000

C 3.166070 1.653625 0.000000

H 0.697051 3.161544 0.000000

H -1.450020 1.652557 0.000000

H -1.499664 -1.167599 -0.889823

H -0.259374 -2.082496 -0.000000

H -1.499664 -1.167599 0.889823

C 4.064794 0.416638 0.000000

H 3.369026 2.249547 -0.889823

H 3.369026 2.249547 0.889823

C 5.530829 0.850897 0.000000

H 3.863035 -0.179691 0.889823

H 3.863035 -0.179691 -0.889823

C 6.429553 -0.386090 0.000000

H 5.733785 1.446820 0.889823

H 5.733785 1.446820 -0.889823

C 7.895588 0.048170 0.000000

H 6.227794 -0.982419 -0.889823

H 6.227794 -0.982419 0.889823

C 8.794312 -1.188817 0.000000

H 8.098544 0.644092 0.889823

H 8.098544 0.644092 -0.889823

H 9.839425 -0.879241 0.000000

H 8.592553 -1.785146 -0.889823

H 8.592553 -1.785146 0.889823

PF_6^- anion:

P 0.000000 0.000000 0.000000

F 1.606000 0.000000 0.000000

F 0.000000 -1.606000 0.000000

F 0.000000 -0.000000 1.606000

F 0.000000 -0.000000 -1.606000

F 0.000000 1.606000 0.000000

```
F -1.606000 -0.000000 0.000000
```

BF_4^- anion:

```
B 0.000000 0.000000 0.000000
F 1.394000 0.000000 0.000000
F -0.465327 -1.314042 0.000000
F -0.465327 0.657021 1.137994
F -0.465327 0.657021 -1.137994
```

2 Parameter Sets

Here, we list the final parameter sets for all force field parametrized in this work.

Table S2: Parameters for $[C_2C_1Im][BF_4]$ model

nonbonded parameters					
site	mass [amu]	charge [e]	σ [Å]	ϵ [kJ/mol]	α [Å^3]
Im	67.070	0.6142	4.673	1.015	5.612
C_1	15.035	0.1481	3.351	1.015	2.068
C_2	29.062	0.2377	4.096	1.015	3.779
BF_4	86.805	-1.0000	4.726	0.601	3.357

bonded parameters	value
Im–C_1 bond	3.409 Å
Im–C_2 bond	3.425 Å
C_2–Im–C_1 angle	139.90°

Table S3: Parameters for $[C_2C_1Im][PF_6]$ model

nonbonded parameters

site	mass [amu]	charge [e]	σ [Å]	ϵ [kJ/mol]	α [Å^3]
Im	67.070	0.6142	4.678	1.008	5.612
C_1	15.035	0.1481	3.354	1.008	2.068
C_2	29.062	0.2377	4.101	1.008	3.779
PF_6	144.964	-1.0000	5.261	0.683	4.653

bonded parameters

	value
Im–C_1 bond	3.409 Å
Im–C_2 bond	3.425 Å
C_2–Im–C_1 angle	139.90°

Table S4: Parameters for $[C_4C_1Im][BF_4]$ model

nonbonded parameters

site	mass [amu]	charge [e]	σ [Å]	ϵ [kJ/mol]	α [Å^3]
Im	67.070	0.6344	4.589	1.175	5.693
C_1	15.035	0.1508	3.293	1.175	2.103
C_4	57.115	0.2148	5.010	1.175	7.409
BF_4	86.805	-1.0000	4.637	0.674	3.357

bonded parameters

	value
Im–C_1 bond	3.489 Å
Im–C_4 bond	4.352 Å
C_4–Im–C_1 angle	130.36°

Table S5: Parameters for $[C_4C_1Im][PF_6]$ model

nonbonded parameters

site	mass [amu]	charge [e]	σ [Å]	ϵ [kJ/mol]	α [Å^3]
Im	67.070	0.6344	4.585	1.180	5.693
C_1	15.035	0.1508	3.290	1.180	2.103
C_4	57.115	0.2148	5.006	1.180	7.409
PF_6	144.960	-1.0000	5.152	0.775	4.653

bonded parameters

	value
Im–C_1 bond	3.489 Å
Im–C_4 bond	4.352 Å
C_4–Im–C_1 angle	130.36°

Table S6: Parameters for $[C_6C_1Im][BF_4]$ model

nonbonded parameters

site	mass [amu]	charge [e]	σ [Å]	ϵ [kJ/mol]	α [Å^3]
Im	67.079	0.6242	4.585	1.200	5.751
C_1	15.040	0.1474	3.291	1.200	2.126
C_6	85.170	0.2284	5.713	1.200	11.128
BF_4	86.805	-1.0000	4.630	0.681	3.357

bonded parameters

	value
Im–C_1 bond	3.486 Å
Im–C_6 bond	4.666 Å
C_6–Im–C_1 angle	128.31°

Table S7: Parameters for $[C_6C_1Im][PF_6]$ model

nonbonded parameters					
site	mass [amu]	charge [e]	σ [Å]	ϵ [kJ/mol]	α [Å^3]
Im	67.079	0.6242	4.584	1.201	5.751
C_1	15.040	0.1474	3.290	1.201	2.126
C_6	85.170	0.2284	5.712	1.201	11.128
PF_6	144.964	-1.0000	5.147	0.779	4.653

bonded parameters	value
Im–C_1 bond	3.486 Å
Im–C_6 bond	4.666 Å
C_6–Im–C_1 angle	128.31°

3 Sensitivity of coarse-grained charge assignment to molecular structure

Many internal degrees of freedom are not treated explicitly in our coarse-grained force fields. One of these is the rotation around the N-C bond, where the carbon atom belongs to the butyl side chain. The bond rotation is indicated in Fig. S2. This torsional degree of freedom is important in describing the liquid structure of alkyl-imidazolium ionic liquids.[S3,S4] We generated structures starting from the minimum energy structure of $C_4C_1Im^+$ by rotating the butyl group around the dihedral axis without re-optimization. The density-derived atomic point charges[S5] were then summed over individual interaction sites and the values are shown in Fig. S2 (colored dots). The change in mean charge on the interaction site is smallest for the methyl-group, and larger and comparable to each other for imidazolium and butyl groups. Charges on imidazolium- and butyl-group anti-correlate. Strongest deviations from the mean are observed for torsional angles where the butyl group points out of the imidazolium plane. These deviations can in part also be attributed to missing structural relaxation. In the CG representation, the torsion is abstracted into a rotation of the whole structure about

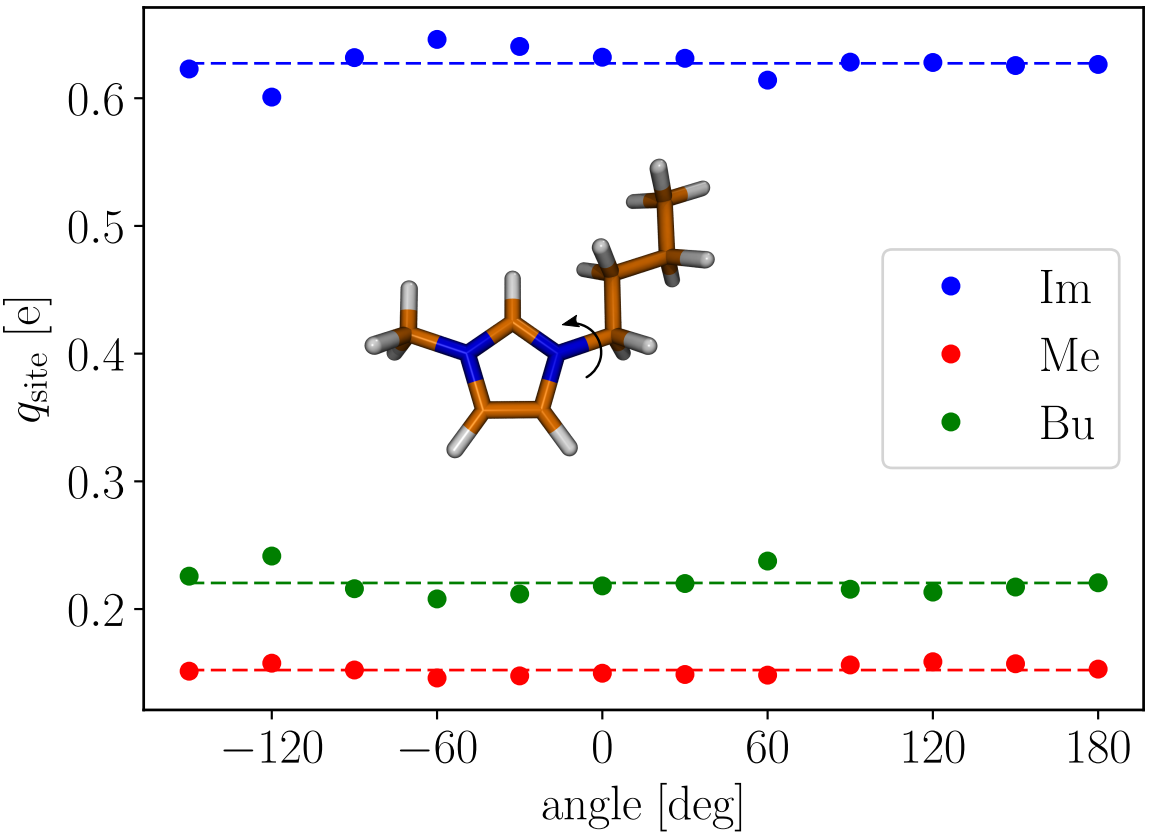

Figure S2: Charge on coarse-grained beads when scanning along dihedral angle along the bond connecting butyl- and imidazolium group, as indicated in the figure. The structure is shown for a dihedral angle of 180°. Charges on the imidazolium group are in blue, on the methyl group in red, and for butyl group in green. The respective averages are shown as dashed lines.

its methyl-imidazolium axis. But, as the torsion influences the charge distribution only marginally, we can conclude that there is merit to this rather abstract coarse-grained model representation.

We furthermore conducted atomistic molecular dynamics simulations of $[C_4C_1Im][PF_6]$ at 350 K using the CL&P force field.[S1,S2] Figure. S3 shows the combined distributions of distance between centers of mass of butyl and imidazolium groups and the angle between methyl, imidazolium and butyl groups. The butyl chain shows a bimodal distribution with respect to the distance between butyl and imidazolium group and a broad peak with a

significant shoulder with respect to the methyl-imidazlium-butyl angle. In the majority of cases, the butyl group is in a configuration similar to our rigid, coarse-grained model. This flexibility could in principle be modelled, but would require additional intramolecular

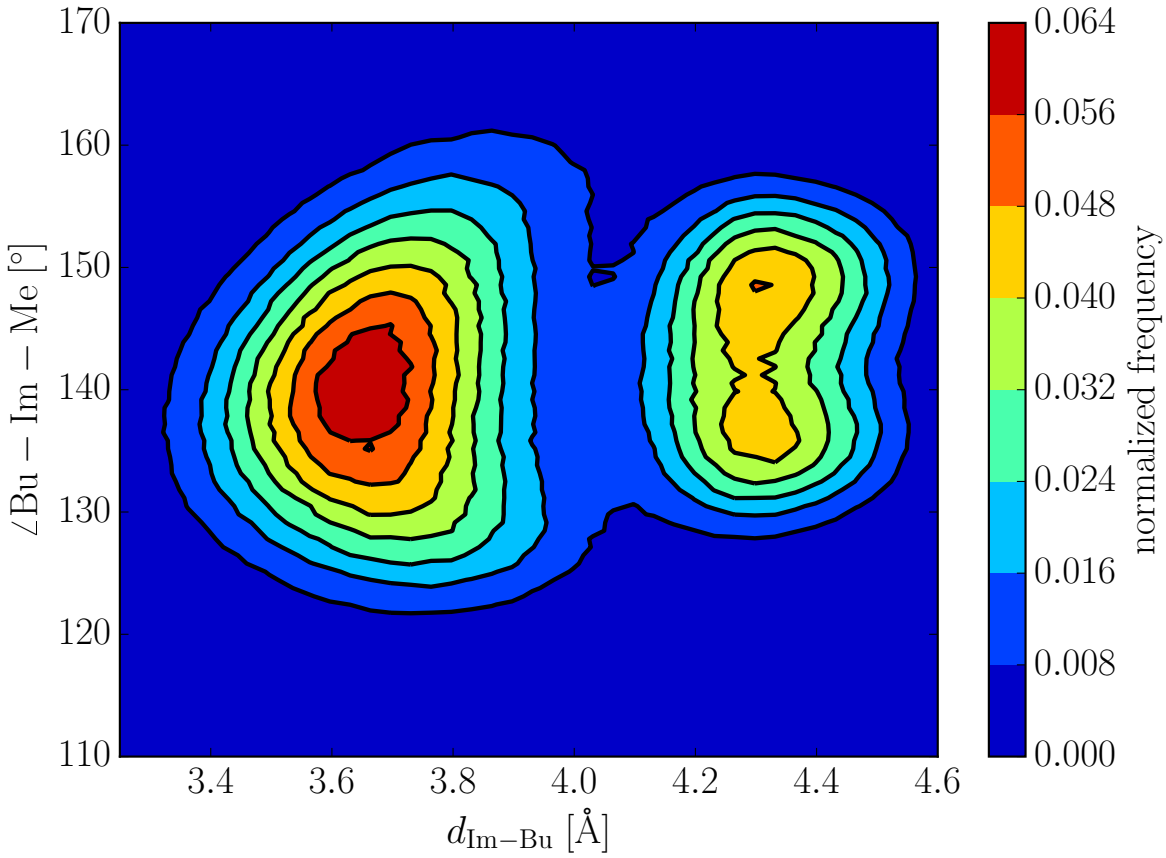

Figure S3: Combined distributions of distance between centers of mass of butyl group and imidazolium group, and angles between centers of mass methyl, imidazolium and butyl groups.

parameters describing the angular distribution. The distance between imidazolium and methyl group is not shown, because it does not show a clear bimodal structure, but rather a single symmetric distribution around an average of 3.6 Å with a standard deviation of 0.1 Å.

4 Liquid structure compared with other force fields

Figure S4 depicts various radial distribution functions (RDFs) from atomistic, and coarse-grained force fields. The RDFs are shown for the atomistic CL&P force field,[S1,S2] the non-polarizable coarse-grained RoyMa force field,[S6] and our CGPol force field. The liquid structure has been calculated for individual coarse-grained interaction sites, and the equivalent centers of mass in the atomistic force fields.

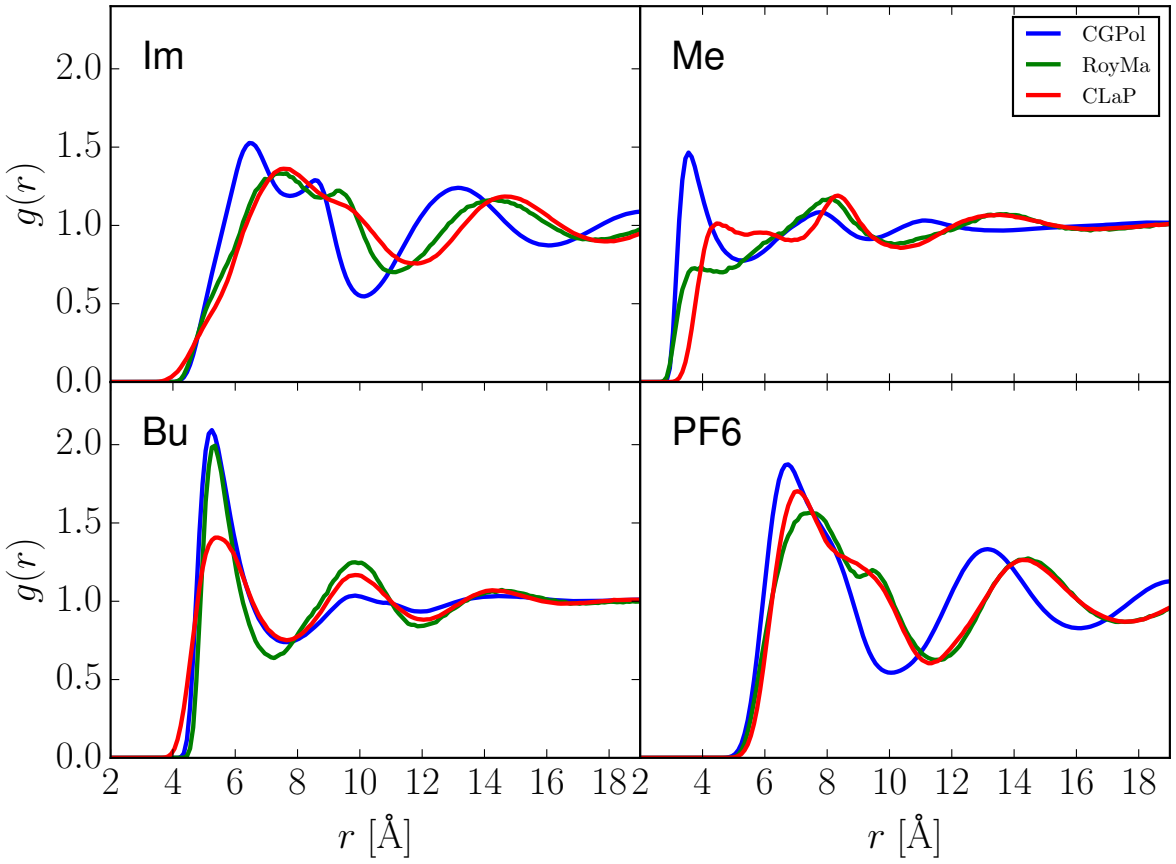

Figure S4: Radial distribution functions $g(r)$ between all interaction sites in coarse-grained models and corresponding all-atom analogues obtained from simulations with coarse-grained, and atomistic force fields. Imidazolium group (Im) top left, methyl (Me) group top right, butyl (Bu) group bottom left, and hexafluorophosphate (PF6) anion bottom right. Radial distribution functions from simulations with CGPol in blue, RoyMa in green, and CL&P in red. Individiual groups are represented by their respective centers of mass.

As explained in the main text, the effective size of our coarse-grained representations is smaller than those of the CL&P and RoyMa force fields. This can be seen here as well, in the RDFs between methyl-, imidazolium-, and hexafluorophosphate groups. The size of the butyl groups is roughly the same between the different force fields. Larger deviations in structure can be observed for the methyl-methyl group RDF. Here, our CGPol force field shows a more pronounced structuring.

5 Example mean square displacement

Figure S5 shows an exemplary mean square displacement in a double-logarithmic plot for $[C_4C_1Im][PF_6]$ to demonstrate the linearity for large t. The ballistic, short-time regime is hardly identifiable due to limit data resolution.

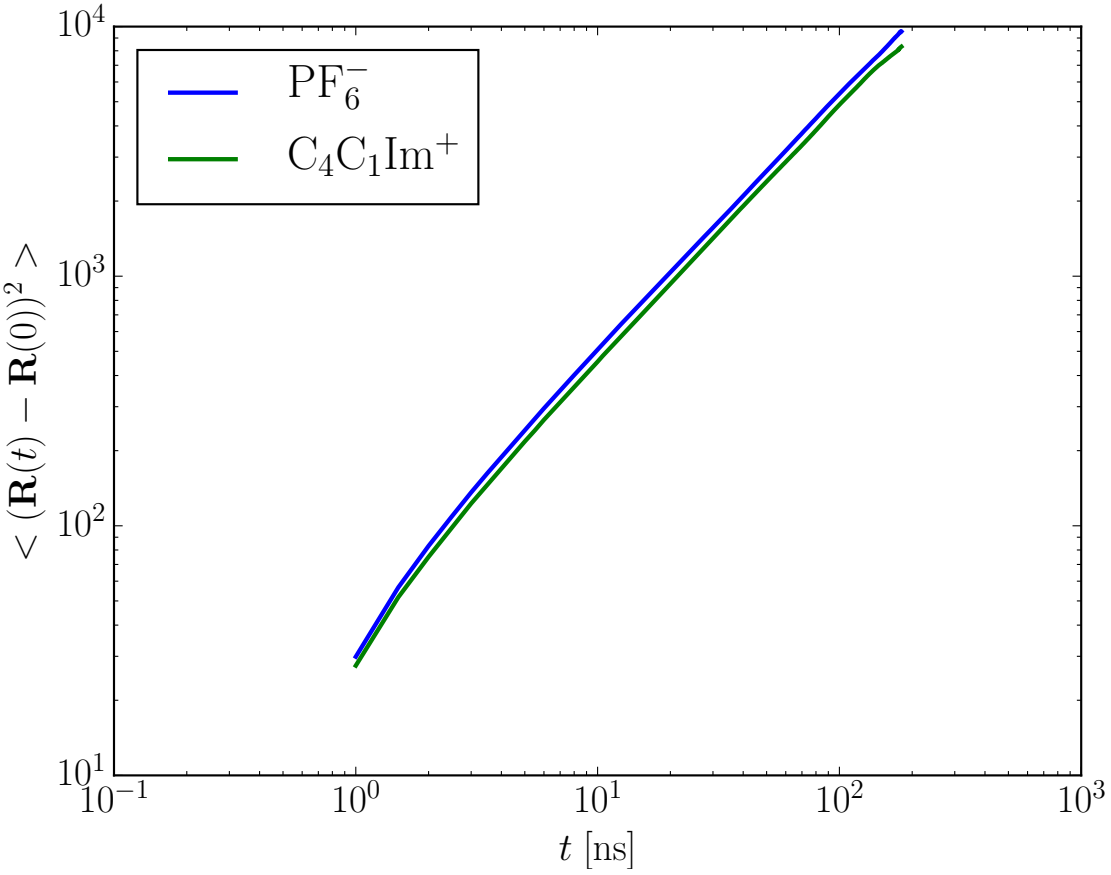

Figure S5: Mean squared displacements $< (\boldsymbol{R}(t) - \boldsymbol{R}(0))^2 >$ for $C_4C_1Im^+$ cation and PF_6^- anion in the ion liquid $[C_4C_1Im][PF_6]$ at 350K.

6 Enthalpies of vaporization

Enthalpies of vaporization were calculated as described in the main text. In table S8 we list the enthalpies of vaporization for all our newly parametrized force fields, together with experimental data and other simulation data.

Table S8: Enthalpies of vaporization for different alkyl chain lengths, compared to experiment (exp.)[S7] and other simulation data from an atomistic, polarizable force field (AApol).[S8] Errors are about 6-7 kJ/mol.

	CGPol (350 K)	exp (298 K)	AApol
$[C_2C_1Im][BF_4]$	122	139, 136	117
$[C_2C_1Im][PF_6]$	118	N/A	131
$[C_4C_1Im][BF_4]$	114	128, 141	120
$[C_4C_1Im][PF_6]$	113	155	129
$[C_6C_1Im][BF_4]$	108	145	126
$[C_6C_1Im][PF_6]$	110	140	131

All values are of the correct order of magnitude, but the ordering between individual species is not described well. However, all values, experimental and theoretical are quite close to each other.

7 Electrical conductivities

The electrical conductivities are reported in the main text. Here, we show the mean square displacements κt of all charges carries in solution, given as:

$$\kappa t = \frac{1}{6Vk_{\mathrm{B}}T} \sum_{i}^{n} \sum_{j}^{n} \left\langle \left(q_i \left[\boldsymbol{R}_i(t) - \boldsymbol{R}_i(0)\right]\right) \left(q_j \left[\boldsymbol{R}_j(t) - \boldsymbol{R}_j(0)\right]\right) \right\rangle . \tag{1}$$

Figure S6 shows the corresponding data for all our parametrized force fields (full lines). The conductivity κ can be extracted from these curves by performing linear regressions (dashed lines in Fig. S6). The linear regression analysis is only valid in the diffusive regime, which is difficult to identify in these data. Hence, the relative errors of this analysis can be quite large (up to 50 %). The fits were conducted in the region depicted in Fig. S6 starting from about 10 ns. Qualitative trends reported in the main text are, however, clearly visible in Fig. S6.

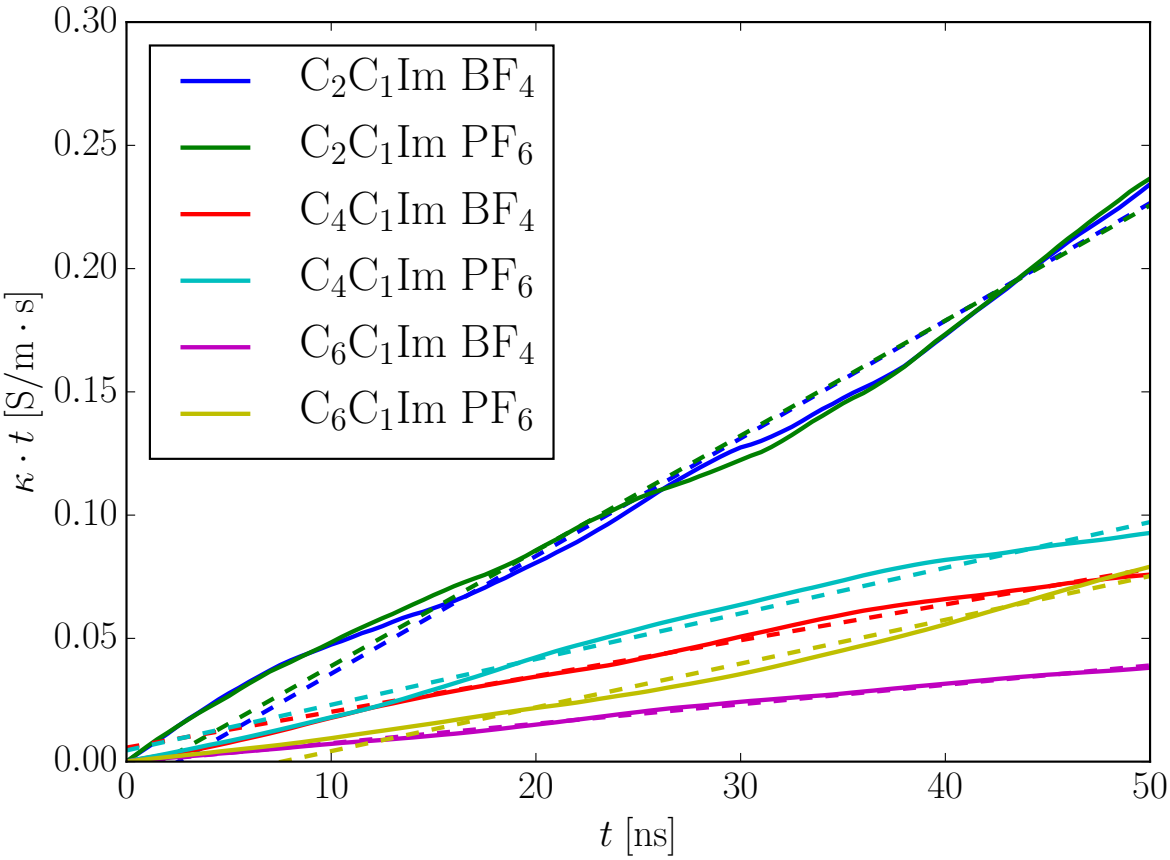

Figure S6: Full mean squared displacement $\kappa \cdot t$ of all ions in coarse-grained molecular dynamics simulations as a function of t, for the calculation of electrical conductivities. The formula for κ is given in eq. 1

8 Example input files

For reproducibility, an example input file for the simulation of $[C_4C_1Im][PF_6]$ with LAMMPS is given below:

```
units real

boundary p p p


atom_style full
```

```
bond_style harmonic
angle_style harmonic
special_bonds lj/coul 0.0 0.0 0.5

read_data data.pol

pair_style lj/cut/thole/long 2.0 12.0
pair_modify tail yes
kspace_style pppm 1.0e-4

pair_coeff 1 1 0.282027 4.585000 5.693 # Im Im
pair_coeff 2 2 0.282027 5.006000 7.409 # Bu Bu
pair_coeff 3 3 0.282027 3.290000 2.103 # Me Me
pair_coeff 4 4 0.185229 5.152000 4.653 # PF6 PF6
pair_coeff 5 5 0.000000 0.000000 5.693 # Im Im
pair_coeff 6 6 0.000000 0.000000 7.409 # Bu Bu
pair_coeff 7 7 0.000000 0.000000 2.103 # Me Me
pair_coeff 8 8 0.000000 0.000000 4.653 # PF6 PF6

group ATOMS type 1 2 3 4
group CORES type 1 2 3 4
group DRUDES type 5 6 7 8
group BMIM type 1 2 3
group PF6 type 4

fix DRUDE all drude C C C C D D D D
```

```
variable nsteps equal 40000000
variable nprint equal ${nsteps}/400000
variable ndump equal ${nsteps}/40000
variable nrestart equal ${nsteps}/40

variable TK equal 350
variable TDK equal 1.0
variable PBAR equal 1.0

neighbor 4.0 bin

timestep 5.

velocity ATOMS create ${TK} 12345
velocity ATOMS zero linear
velocity DRUDES create 0 666

compute TATOM ATOMS temp/com

fix PSTAT ATOMS npt temp ${TK} ${TK} 500 iso ${PBAR} ${PBAR} 5000
fix_modify PSTAT temp TATOM press thermo_press

fix ASPC DRUDES aspc/drude 2 0.6 1000

fix SHK ATOMS rattle 1.e-04 100 0 a 1 b 1 2

fix MOM all momentum 100 linear 1 1 1 rescale
```

```
thermo_style custom step etotal ke pe ebond evdwl ecoul elong press vol c_
   TATOM
thermo ${nprint}

dump TRJ all custom ${ndump} dump.lammpstrj id element xu yu zu
dump_modify TRJ element Im Bu Me P D D D D sort 1

restart ${nrestart} restart.*.lmp

run ${nsteps}

write_restart restart.*.lmp
write_data data.*.lmp
```

References

(S1) Canongia Lopes, J. N.; Deschamps, J.; Pádua, A. A. H. Modeling Ionic Liquids Using a Systematic All-Atom Force Field. *J. Phys. Chem. B* **2004**, *108*, 2038–2047.

(S2) Canongia Lopes, J. N.; Pádua, A. A. H. CL&P: A generic and systematic force field for ionic liquids modeling. *Theor. Chem. Acc.* **2012**, *131*, 1129.

(S3) Hunt, P. A.; Gould, I. R. Structural Characterization of the 1-Butyl-3-methylimidazolium Chloride Ion Pair Using ab Initio Methods. *J. Phys. Chem. A* **2006**, *110*, 2269–2282, PMID: 16466265.

(S4) Koßmann, S.; Thar, J.; Kirchner, B.; Hunt, P. A.; Welton, T. Cooperativity in ionic liquids. *J. Chem. Phys.* **2006**, *124*, 174506.

(S5) Blöchl, P. E. Electrostatic decoupling of periodic images of plane-wave-expanded densities and derived atomic point charges. *J. Chem. Phys.* **1995**, *103*, 7422–7428.

(S6) Roy, D.; Maroncelli, M. An Improved Four-Site Ionic Liquid Model. *J. Phys. Chem. B* **2010**, *114*, 12629–12631.

(S7) Zaitsau, D. H.; Kabo, G. J.; Strechan, A. A.; Paulechka, Y. U.; Tschersich, A.; Verevkin, S. P.; Heintz, A. Experimental Vapor Pressures of 1-Alkyl-3-methylimidazolium Bis(trifluoromethylsulfonyl)imides and a Correlation Scheme for Estimation of Vaporization Enthalpies of Ionic Liquids. *J. Phys. Chem. A* **2006**, *110*, 7303–7306, PMID: 16737284.

(S8) McDaniel, J. G.; Choi, E.; Son, C. Y.; Schmidt, J. R.; Yethiraj, A. Ab Initio Force Fields for Imidazolium-Based Ionic Liquids. *J. Phys. Chem. B* **2016**, *120*, 7024–7036.